Mon. Not. R. Astron. Soc. **327,** 949–954 (2001)

A *z*-invariant Rayleigh beacon wavefront sensor

R. Ragazzoni,[1] M. Tordi,[1★] E. Diolaiti[2,3] and D. Kirkman[4]
[1]*Astronomical Observatory of Padova, vicolo dell'Osservatorio 5, I–35122 Padova, Italy*
[2]*Department of Astronomy, vicolo dell'Osservatorio 2, University of Padova, Italy*
[3]*Department of Astronomy via Ranzani 4, University of Bologna, Italy*
[4]*Center for Astrophysics and Space Science, University of California, San Diego, CA 92037-0421, USA*

Accepted 2001 June 25. Received 2001 June 23; in original form 2001 February 22

ABSTRACT

An innovative concept of wavefront sensing for Rayleigh beacons is introduced along with an example of a possible wavefront sensor. This new approach does not require the gating technique to limit the useful range of the laser source and therefore looks simpler to implement than previous Rayleigh concepts, and may additionally allow more efficient use of the photons emitted by the Rayleigh beacon. Our technique is based upon an optical element in the focal plane area whose section does not change for the conjugation of different ranges from the telescope aperture, hence the name *z*-invariant. The wavefront sensor shown here is an example of this new class. It is a compact pupil-plane wavefront sensor and as such allows for a layer-oriented configuration. It is shown that its sensitivity, while higher than usual gating approaches, is far from the possible limits leading us to speculate that other *z*-invariant wavefront sensors can reach much larger efficiencies.

Key words: instrumentation: adaptive optics – instrumentation: miscellaneous.

1 INTRODUCTION

In order to overcome the sky coverage limitation of adaptive optics (Beckers 1993) one can use artificial reference beacons generated by laser light launched from the ground by, or near, the observing telescope (Foy & Labeyrie 1985). This is not the only possible solution; other options range from the use of only natural guide stars embracing a large field of view probably attainable only with much larger telescopes than the current 10-m class generation (Ragazzoni 1999; Ragazzoni, Farinato & Marchetti 2000), the excitation of the atmosphere by means of radio waves (Ribak 1998), to the installation of a reference source aboard satellites with an orbit that allows only a very small apparent proper motion (Baddiley & Greenaway 1992). However, the most popular approach by far is the use of laser guide stars (LGSs hereafter) by means of a ground-based laser projector that is able to give a significant photon return from a given altitude with some sort of physical process (Gardner, Welsh & Thompson 1990). So far just two ways have been thought of, namely back-scattering resonance in the natural sodium layer at an altitude of approximately 92 km (Foy & Labeyrie 1985; Happer et al. 1994) and Rayleigh scattering in the lower portion of the atmosphere. At first glance the sodium LGSs are superior: they occur at a higher altitude than that attainable with a Rayleigh beacon and, because of the limited thickness of the sodium layer they can be, as a first approximation and for relatively small telescopes, treated as a thin slab, hence producing a nearly point reference. Most of the disadvantages of LGSs, like the lack of tip–tilt information (Pilkington 1987; Rigaut & Gendron 1991) and light pollution in the launching area, are common to both sodium and Rayleigh types. In contrast to the sodium LGS the Rayleigh beacon is not localized at a specific altitude. A straightforward approach is to *gate* the returning signal by generating the LGS with a pulsed beacon having a pulse format suitable for such a purpose (Fugate et al. 1991). Continuous gating and/or multiple gating can be introduced at the expense of a substantial optomechanical complication (Ragazzoni 2000). Adaptive optics systems equipped with Rayleigh LGSs in gating mode have also already produced scientific results (Drummond, Christou & Fugate 1995; Spinhirne et al. 1998). The other main difference is inherent in the type of physical process involved in order to get some reasonable photon return. Because of the resonant back-scattering nature of the sodium LGS it is mandatory for this artificial beacon to be generated by a laser exactly tuned to the sodium doublet wavelengths. Rayleigh LGSs, on the other hand, can be generated by a laser of any wavelength, with some preference to the shorter wavelength because of the larger photon return (the latter being proportional to λ^{-4}) to be balanced against the transparency of the atmosphere at the shorter wavelengths. Unfortunately there are no known lasers that *naturally* emit at the proper sodium resonance frequency and, moreover, the (still partially unknown) features of the sodium layer, mainly its saturation characteristics (Milonni, Fugate & Telle 1998), make easy generation of sodium LGSs a difficult task. Scaling to larger power and to larger telescopes is another issue that, if not against

★E-mail: tordi@pd.astro.it

sodium LGSs, is at least able to reconduct the comparison with Rayleigh on a more common ground. For a $D = 100$-m class telescope (Gilmozzi et al. 1998; Mountain & Gillet 1998), in fact, perspective enlargement (Beckers 1992) of a sodium spot will lead, as will be shown in the next section, to an apparent angular size of the order of 10 arcsec, at least at the edge of the pupil and in the radial direction. A Shack–Hartmann approach to sense such a huge spot with a precision of the order of the resolving power in the visible range of such a telescope (being of the order of one milliarcsec) needs a centroiding accuracy with a precision of the order of one part over 10^4, a task to be accomplished with the formidable number of $N \approx 10^8$ photons per subaperture per integration time. Since this is even greater than the full well of currently available fast charge-coupled devices (CCDs) it is expected that one should treat sodium beacons as elongated and, when a pulsed laser is used, the temptation will be to use some gating technique very similar to those used with Rayleigh beacons. Moreover, one should take into account that saturation effects in the sodium layer will occur and it is likely that the required power to obtain such a photon return will be unrealistic.

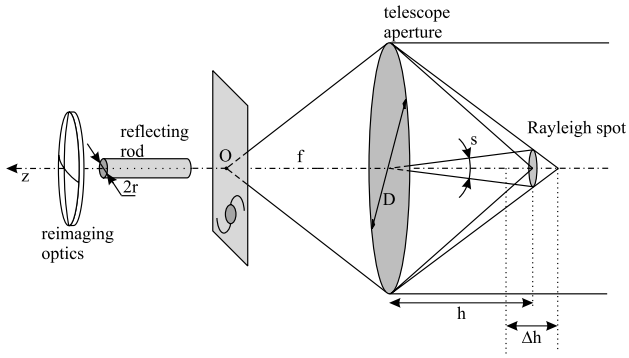

Figure 1. In a Rayleigh LGS one can *gate* the returning pulse corresponding to a certain range interval Δh. The larger such a figure, the larger the photon return. However, a large Δh also produces some unacceptable enlargement of the spot as seen from the telescope and a trade-off is required in order to have such a defocus smaller than the beacon angular size s. In the figure we also show the main component of the proposed wavefront sensor: from right to left, a LGS, a telescope, a reflecting rod and re-imaging optics. While an all centred and coaxial system (including the Rayleigh LGS) is shown here, the considerations carried out in the text do not rely on this particular configuration.

2 RAYLEIGH LGS EFFICIENCY

Let us consider a telescope of diameter D looking at a Rayleigh beacon gated to an average range h and extending for a Δh span (see also Fig. 1). Let us also assume that the LGS is launched from a co-axial projector leading to an angular spreading s of the ascending beam. Points along the axis of the column will exhibit a certain angular broadening, because they are defocused with respect to the h ranged mid-point. It is reasonable to impose the condition that such a broadening is to be limited to roughly the same angular size s. Assuming that one is using a Shack–Hartmann wavefront sensor (WFS) to look at the gated Rayleigh scattered light, a larger angular size, related to a wider extension of the beacon along the optical axis, will lead to a proportionally greater number of photons, with a roughly linear trend. On the other hand, the range of the gated beacon can be expressed as

$$\Delta h \approx \frac{2sh^2}{D}. \tag{1}$$

In order to avoid adaptive optics compensation in the launching projector it is reasonable to consider that $s \approx \lambda/r_0$ and equation (1) becomes

$$\frac{\Delta h}{h} \approx \frac{2h\lambda}{Dr_0}. \tag{2}$$

Using $D = 10$ m, $h = 30$ km, $\lambda = 500$ nm and $r_0 = 0.2$ m one gets $\Delta h/h \approx 0.015$. In principle the light coming back to the ground is just hampered by such a factor (assuming, for comparison, that a large fraction of the Rayleigh column could be, in principle, used, or in other words comparing with $\Delta h/h \approx 1$). While the calculation carried out is a sort of orders of magnitude estimate it is clear that with the simple gating approach a large part of the light is essentially wasted. In the following we introduce and discuss a novel class of WFS which is able to cope with the intrinsic nature of the Rayleigh beacon and can use most of the returning photons without any moving parts. It is noticeable that the attainable gain, just in terms of collected photons, is of the order of $h/\Delta h$ as given by the inverse of equation (2). This amounts to a couple of orders of magnitude for a $D = 10$-m class telescope and rises to three orders of magnitude for a $D = 100$-m class telescope. Thus, even if new methods make inefficient use of the collected photons they can realize very large efficiency gains with respect to gated systems.

3 SYSTEM SET UP

A schematic set up of the system is shown in Fig. 1. The wavefront sensing device consists of a reflecting rod of radius r and a re-imaging optical element. While the useful range of the guide star is $h \pm \Delta h/2$ as in the simple gating approach we do not place any limit on the $\Delta h/h$ figure. The optical axis of the system, pointing at the image plane, is denoted by z; its origin is located at the focus of an infinitely distant source. The LGS is at a finite range from the telescope aperture, so it will be imaged at $z > 0$. After introducing a reference frame (x, y) on the aperture plane of the telescope, we define the normalized polar coordinates (ρ, θ), where $\epsilon \leq \rho \leq 1$ and ϵ is the radius of the central obstruction in units of the aperture radius. The exit pupil of the telescope is represented in Fig. 2, where it is located at $-z_p$. In all our considerations we will assume $z_p = \infty$: the rays coming from a given point on the pupil appear parallel as seen from the wavefront sensing zone. With no atmospheric turbulence the wavefront emitted by the LGS and incident on the telescope aperture has an ideal spherical shape. Under the geometric optics approximation the reflecting rod and the re-imaging optics form an image of the exit pupil (Fig. 2). This is accomplished without any wavefront perturbation. In the more general case we investigate how the brightness of the re-imaged pupil will change, in order to find out any useful relationship that can be used to reconstruct the wavefront itself. Because the design of the WFS does not depend upon the z position (the section of the WFS is always a circular one for any relevant value of z) the result will not depend upon the altitude of the spot. In fact the system can work with an unfavourable pulse format or even a continuous wave laser!

4 TURBULENCE AND PUPIL BRIGHTNESS

Let us consider the wavefront distortion in polar coordinates $W(\rho, \theta)$ and consider the effect of wavefront distortion separately

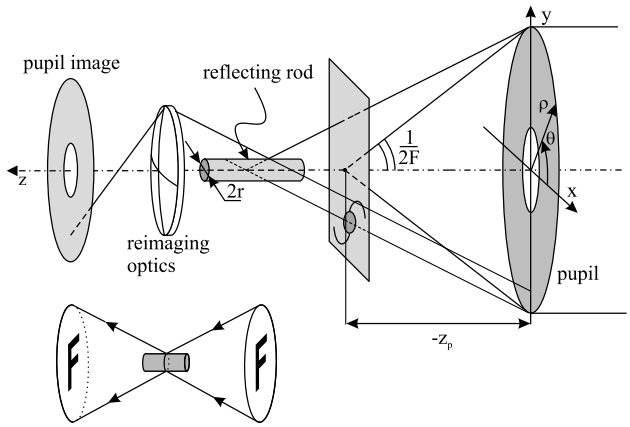

Figure 2. Image of the telescope exit pupil, formed by the rod and the re-imaging optics. In the lower-left inset one can see how an image of the pupil, usually rotated by 180° after an intermediate focal plane, is further rotated by the same amount (leading to a nearly 1:1 re-imaging) by a reflective rod, at least under the assumptions described in the text.

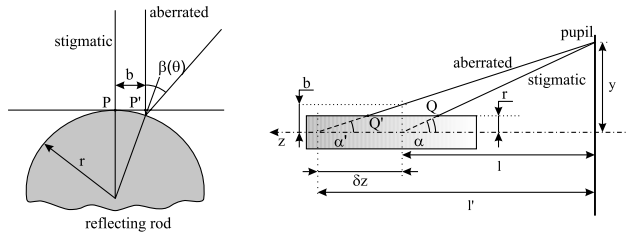

Figure 3. Left panel: effect of an aberration $\partial W/\partial\theta$; the stigmatic and aberrated rays, coming from the same point on the infinitely distant exit pupil, are parallel. Right panel: effect of $\partial W/\partial\rho$; the pupil is at a finite distance.

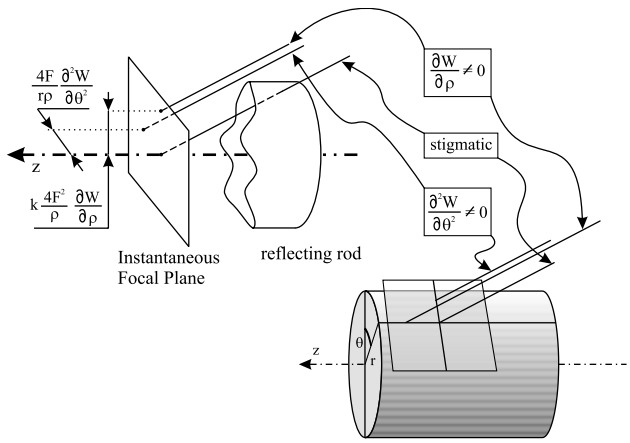

Figure 4. Overall effect as a result of first-order aberrations.

for these two coordinates. Wavefront distortion given by a non-zero $\partial W/\partial\theta$ may be studied considering a ray leaving the exit pupil from a point on the y-axis. If the ray is not aberrated (Fig. 3, left), it falls on the rod at P: the projection of its trajectory on to the (x, y) plane is normal to the rod surface. An aberrated ray leaving the same point on the pupil with a deflection $\partial W/\partial x$ hits the rod at P' and is deviated by an angle β, given by

$$\beta \approx \frac{2b}{r} \tag{3}$$

where b is the length of the segment $\overline{PP'}$ and it is assumed that $b \ll r$. We note that b is proportional to the derivative of the wavefront along the azimuthal angle θ defined over the pupil. Moreover, this proportionality is weighted by a ρ^{-1} factor. Carrying out the calculation we obtain

$$\beta \approx \frac{4F}{\rho r}\frac{\partial W}{\partial \theta}, \tag{4}$$

where $F = f/D$ is the focal ratio of the telescope. Given the symmetry of the problem, it is always possible to apply the considerations above to any point (ρ, θ) on the exit pupil by simply aligning the y-axis with the direction defined by the angle θ. In order to describe the intensity variation on the image of the exit pupil, we consider two rays coming from the points (ρ, θ) and $(\rho, \theta + \mathrm{d}\theta)$. After reflection, θ is mapped to $[\theta + \pi + \beta(\theta)]$ and $(\theta + \mathrm{d}\theta)$ to $[\theta + \mathrm{d}\theta + \pi + \beta(\theta + \mathrm{d}\theta)]$; the angular separation between the rays after reflection is

$$\mathrm{d}\theta' = \mathrm{d}\theta + \beta(\theta + \mathrm{d}\theta) - \beta(\theta) \tag{5}$$

and expanding $\beta(\theta + \mathrm{d}\theta)$ to first order according to equation (3) one obtains

$$\mathrm{d}\theta' \approx \mathrm{d}\theta + \frac{4F}{\rho r}\frac{\partial^2 W}{\partial^2 \theta}\mathrm{d}\theta. \tag{6}$$

The transformation $\mathrm{d}\theta \rightarrow \mathrm{d}\theta'$ is associated with a modification of the area element and, consequently, of the ray density on the image of the exit pupil. The ratio between the aberrated and the non-aberrated brightness in a neighbourhood of (ρ, θ), denoted by I' and I respectively, is therefore equal to the inverse ratio of the area elements:

$$\frac{I'}{I} \approx 1 - \frac{4F}{\rho r}\frac{\partial^2 W}{\partial^2 \theta}. \tag{7}$$

The effect of a wavefront distortion $\partial W/\partial\rho$ on a ray leaving the exit pupil from a point (ρ, θ) may be evaluated again by aligning the y-axis along the direction identified by the angular coordinate θ. In the absence of turbulence the ray is reflected at Q (Fig. 3, right); the aberrated ray exits the pupil with a deflection $\gamma = \partial W/\partial y$ and hits the rod at Q'. In the approximation of an infinitely distant exit pupil we can assume $\alpha \simeq \rho/(2F)$ and, since typically $F \sim 10$, the angle α may be assumed to be small; therefore the displacement $\overline{QQ'} \approx \delta z$ is

$$\delta z \simeq l' - l \simeq \frac{y}{\alpha} - \frac{y}{\alpha - \gamma} \simeq \frac{4F^2}{\rho}\frac{\partial W}{\partial \rho}. \tag{8}$$

If we assume that the aberration $\partial W/\partial\rho$ does not change over an infinitesimal distance $\mathrm{d}\rho$ along the y-axis on the pupil, we have no observable effect. We can make the device sensitive to the aberration by introducing a non-uniform reflectivity of the rod surface along the optical axis. Let us assume, for instance, that such a reflectivity law is given by

$$\frac{I_\mathrm{r}}{I_\mathrm{i}} = \exp(-kz), \tag{9}$$

where I_i and I_r are the incident and the reflected intensities. In this way the aberration $\partial W/\partial\rho$ introduces a brightness modulation on the image of the exit pupil given by

$$\frac{I'}{I} = \frac{\exp[-k(z + \delta z)]}{\exp(-kz)} \tag{10}$$

where, again, I' and I refers to the brightness in the reimaged pupil

with and without the wavefront deformation considered here. Assuming that the effect of the aberration is small we can modify the right side of equation (10) using the approximation $\exp(\epsilon) \approx 1 + \epsilon$, and by using equation (8) one has

$$\frac{I'}{I} \approx 1 - k\frac{4F^2}{\rho}\frac{\partial W}{\partial \rho}. \tag{11}$$

Finally one can write the combined effect of the aberrations along θ and ρ as (see Fig. 4)

$$I = I_0\left(1 - \frac{4F}{r\rho}\frac{\partial^2 W}{\partial \theta^2}\right)\left(1 - k\frac{4F^2}{\rho}\frac{\partial W}{\partial \rho}\right) \tag{12}$$

where I_0 is the brightness illumination of the pupil. Modifying the above equation and neglecting the highest order, cross terms, one finally obtains

$$I = I_0\left(1 - \frac{4F}{r\rho}\frac{\partial^2 W}{\partial \theta^2} - k\frac{4F^2}{\rho}\frac{\partial W}{\partial \rho}\right). \tag{13}$$

We note that the latter depends upon the Laplacian of the highest layers (Ribak 1998) or in other words on scintillation.

5 PERFORMANCE EVALUATION WITH FINITE SPOT SIZE

In the calculations carried out in the preceding section r can be made arbitrarily small and k can be made arbitrarily large in order to give to the WFS any realistic sensitivity. This statement is true only within the assumptions made to carry out the previous calculation and, generally speaking, is not correct. Both r and k have to fulfil some conditions that translate into some limits on the sensitivity of the rod WFS. We note that because of the finite size of the Rayleigh beacon unaberrated rays will embrace a physical size at the rod place and (see also Fig. 5) they will be reflected in a way to re-image a point on the pupil as a finite extent arc. While we ignore that such an arc will not be uniformly illuminated we can impose the condition that the physical displacement on the pupil is to be smaller than r_0 in order to retain a re-imaging of the pupil useful for adaptive optics purposes.

Assuming, as already mentioned in Section 2, $s \approx \lambda/r_0$ the angle

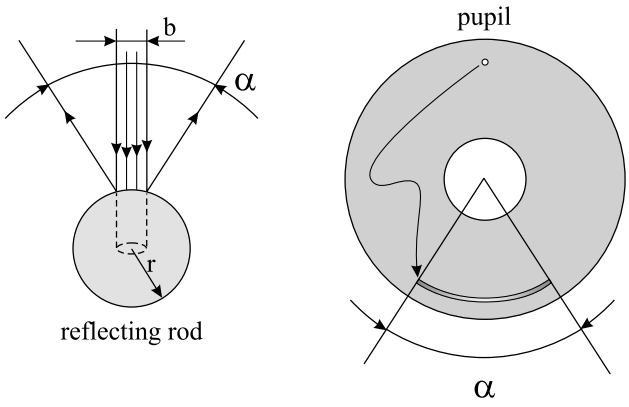

Figure 5. A spot size of physical size b will produce a non-stigmatic pupil re-imaging on to the wavefront sensor detector (left). In fact a point will be spread over an arc on the pupil (right). This poses limits on the radius r in order to avoid the arc being larger than r_0.

α will be given by

$$\alpha \approx 2\frac{\lambda f}{r r_0}. \tag{14}$$

In the worst case (at the edge of the telescope) such an angular displacement will produce a physical broadening of the order of $\alpha D/2$. Limiting such a displacement equal to r_0 leads to a minimum rod radius $r_{\min}$ given by

$$r_{\min} = \frac{Df\lambda}{r_0^2}. \tag{15}$$

This figure, used in equation (7), leads to a certain sensitivity for the angular variations of W. We now assume that the same sensitivity is retained for the radial part. Let us check the resulting figure for k. It is to be pointed out, in fact, that the Rayleigh beacon will extend over the z-axis in the wavefront sensing area for a portion l given by

$$l = \Delta h\left(\frac{f}{h}\right)^2. \tag{16}$$

Such a value is to be compared with k^{-1}. In fact a much smaller figure for the latter would essentially translate into a subtle form of *gating* and no real advantage would be obtained. To be more precise the overall efficiency in the reflectivity from the rod will be given by

$$\eta = \frac{1}{kl}(1 - \mathrm{e}^{-kl}). \tag{17}$$

Assuming that the two terms in equation (13) have similar gain one obtains

$$\frac{4F}{r\rho} \sim k\frac{4F^2}{\rho} \tag{18}$$

which, solved for k^{-1}, gives

$$k^{-1} = \left(\frac{D}{r_0}\right)^2 \lambda F^2. \tag{19}$$

A direct comparison with l can be given by evaluating the adimensional product:

$$lk = \frac{\Delta h}{h^2}\frac{r_0^2}{\lambda}. \tag{20}$$

It is noticeable that such a term is of the order of unity for reasonable choices of the various terms. Generally speaking the sensitivity of this WFS is rather low with respect to what one could obtain with other approaches. A one-wavelength variation across the wavefront will generate an intensity variation (where 'ng' refers to the non-gating case) given by

$$\frac{\Delta I_{1\lambda}^{\mathrm{rod}}}{I_{\mathrm{ng}}} = 4\eta\left(\frac{r_0}{D}\right)^2, \tag{21}$$

a rather low figure, indeed. However, the absence of any gating allows the measurement over a long range of the Rayleigh beacon. Let us assume for this case $\Delta h \approx h$, hence, recalling equation (2) the ratio between the light usable by a gated Shack–Hartmann with respect to the class of WFSs described here is just

$$\frac{I_{\mathrm{g}}}{I_{\mathrm{ng}}} \approx \frac{(\Delta h/h)_{\mathrm{g}}}{(\Delta h/h)_{\mathrm{ng}}} \approx \frac{2h\lambda}{Dr_0} \tag{22}$$

where the prefix 'g' refers to the gating case. In a Shack–Hartmann

WFS the variation of intensity in the quad cells, when a single wavelength aberration is introduced, is of the order of

$$\frac{\Delta I_{1\lambda}^{\mathrm{SH}}}{I_{\mathrm{g}}} = \frac{r_0}{D}. \tag{23}$$

Assembling the last equations together one can derive the effective gain G of using the Rayleigh beacon in a non-gated configuration with the z-invariant WFS described in this paper:

$$G = \frac{2\eta r_0^2}{\lambda h}. \tag{24}$$

With some reasonable numbers, like $\eta \approx 0.5$ (leading to $kl \approx 2$) the gain becomes $G \approx 4$. This figure, accepted as it is, shows that there is a marginal advantage in using such a WFS with respect to the traditional ones. However, the detector side or the optomechanics involved (depending upon how the gating is performed) will become greatly simplified.

6 OTHER CONSIDERATIONS

There are a few additional remarks on the rod WFS which we now mention without going into deeper detail. The first one refers to the approximation $z_{\mathrm{p}} = \infty$ introduced in Section 3 and later used throughout the paper. In the case of a limited z_{p} the only effect is to distort radially the shape of the pupil. This means that using a conventional detector (like a CCD) the pupil sampling will be uneven. Moreover the Jacobian of the pupil transformation associated with the re-imaging on to the detector will no longer be flat and a fixed pattern brightness will appear on the pupil plane. In particular, when the exit pupil is much closer than what has been assumed in the previous sections, the internal portion of the pupil will exhibit a larger brightness than average, while the opposite occurs for the outer edge. In practice, this means that the optical design of the relay to convey light on to the reflective rod will have to provide an exit pupil whose distance from the intermediate focal plane is kept over a given threshold. Such a limiting figure is to be properly chosen in such a way that its effects can be properly taken into account without a significant loss in sensitivity. The second aspect concerning this wavefront sensor is the straightforward way in which it can be optically implemented in a layer-oriented configuration (Ragazzoni et al. 2000): several Rayleigh beacons, all extending for a significant portion of their length, are coupled together in more than one detector, each coupled with the proper deformable mirror in a multi-conjugate adaptive optics (MCAO) (Beckers 1989; Ellerbroeck 1994) (see Fig. 6). We note here that scintillation effects on such a WFS will be strongly attenuated, because in MCAO correction scintillation is significantly lower than in classic adaptive optics.

The WFS we have described has a very low efficiency. In fact, assuming that the same overall number of photons are used in each case, the efficiency of this sensor is much less than a Shack–Hartmann and, by a further significant factor, even much less sensitive than a pyramid WFS working with a natural guide star (Ragazzoni & Farinato 1999). This suggests that the solution described so far is not the ultimate solution for the z-invariant WFS class. The main reason for the low sensitivity is that the angular side (or, in other words, with respect to the $\partial W/\partial\theta$ term) relies on the spreading of the light pencil on the edge of the pupil (as illustrated in Fig. 5). One could conceive z-invariant WFSs with other sectional shapes that will not exhibit such a problem. A square section, for instance, will no longer exhibit such a problem,

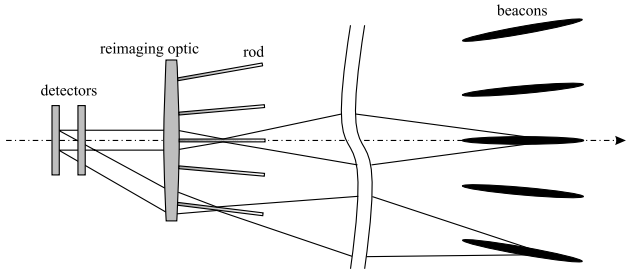

Figure 6. The rod wavefront sensor is a pupil-plane one. In principle one could conceive a system with a set of multiple Rayleigh beacons and several rods coupled to a single large re-imaging optics. The rods could be directly glued to the front surface of the lens. For large FoV, however, the option to sum up the wavefront sensor data in a layer-oriented fashion could be attractive. To keep the picture simple, marginal rays are shown here only for a couple of Rayleigh beacons at a specific range.

but suffers from limitations in the portion of the pupil usable for WFS that would require the pupil light to be split into several beams, leading to an optomechanically complex solution. Other solutions may be more promising and will be investigated. In the case that an efficient and optomechanically simple solution can be found, the way in which the radial part of the wavefront (or, in other words, the $\partial W/\partial\rho$ component) is sensed will likely become the limiting factor for this type of WFS. Some preliminary investigations, assuming a more generalized variation of reflectivity along a generic z-invariant WFS, do not lead to a significant improvement on this side. This suggests that one should be forced to modify the technique used to sense the radial part and/or to modify the invariance of the section for the optical element perturbing the light beam in the focal plane region. This could lead to similar concepts like a section whose similarity is kept over the z direction rather than remaining strictly unchanged. (This comprises, for instance, a conical reflective rod, where the section remains a circular one along z, but its characteristic size and the radius change smoothly.) A generalized analysis of these solutions is, however, beyond the scope of this paper.

7 CONCLUSIONS

In this paper a new class of WFS, named z-invariant here, has been introduced with the example of the reflective rod WFS. It is a very simple optical set up and we have shown with a preliminary but somewhat detailed analysis that it is slightly superior with respect to a traditional gating approach. This work should be placed in the perspective of the various proposals for WFS designed explicitly to sense the atmospheric turbulence using a Rayleigh beacon without *wasting* most of the scattered light. For instance, with respect to the roof prism WFS described elsewhere (Ragazzoni 2000), it is more simple to implement in terms of optomechanical layout, but on the other hand it is more efficient in terms of sensitivity to wavefront deformation. In other words, given a certain number of photons, the rod WFS described here is rather less sensitive with respect to more conventional approaches. This is more than balanced by the possibility of using a large fraction of the Rayleigh scattered beam, so that the approach described, as it is, can be considered as an attractive option. However, we speculate here on the possibility of finding out a somewhat similar technical realization of the general z-invariant concept illustrated here, that could exhibit both a reasonable sensitivity and the usage of most of the Rayleigh scattered photons from a LGS. A further feature that such a WFS should exhibit is, we think, the compactness simplicity of

realization and alignment. Of the three features pointed out (high sensitivity, z-invariance and simple set up) the rod WFS retains only the latter two. The *movie*-like WFS (Angel & Lloyd-Hart 2000; Lloyd-Hart et al. 2000) for instance, while fulfilling the first three conditions, fails to comply with the last two. All these considerations suggest reconsideration of Rayleigh beacons in the light of AO schemes. It is clear, however, that most of the practical considerations outlined here are strongly dependent upon the possibility of achieving reliable, high power, sodium lasers. Experience on the field, from both a conservative and novel concept approach, can only lead to benefit the matter greatly.

ACKNOWLEDGMENTS

Thanks are due for the useful discussions to Piero Salinari, Simone Esposito and Bruno Femenia at the Astrophysical Observatory of Arcetri, Italy.

REFERENCES

Angel J. R. P., Lloyd-Hart M., 2000, SPIE, 4007, 270
Baddiley C. J., Greenaway A. H., 1992, in Mattok C., ed., ESA Conf., Targets for Space-Based Interferometry. ESA Publications Division, Noordwijk, p. 209
Beckers J., 1989, SPIE, 1114, 215
Beckers J., 1992, App. Opt., 31, 6592
Beckers J., 1993, ARA&A, 31, 13
Drummond J. D., Christou J. C., Fugate R. Q., 1995, ApJ, 450, 380
Ellerbroek B., 1994, J. Opt. Soc. Am. A, 11, 783
Foy R., Labeyrie A., 1985, A&A, 152, L29
Fugate R. Q. et al., 1991, Nat, 353, 144
Gardner C. S., Welsh B. M., Thompson L. A., 1990, Proc. IEEE, 78, 1721
Gilmozzi R. et al., 1998, SPIE, 3352, 778
Happer W., MacDonald G. J., Max C. E., Dyson F. J., 1994, JOSA, 11, 263
Lloyd-Hart M., Jefferies S. M., Hege E. K., Angel J. R. P., 2000, SPIE, 4007, 277
Milonni P. W., Fugate R. Q., Telle J. M., 1998, JOSA, 15, 217
Mountain M., Gillet F. C., 1998, Nat, 395, A23
Pilkington J. D. H., 1987, Nat, 330, 116
Ragazzoni R., 1999, A&AS, 136, 205
Ragazzoni R., 2000, in Herbs T., ed., Proc. of Ringberg Conf., Science with LBT. Neumann Druck, MPI f. Astron., Heidelberg, p. 13
Ragazzoni R., Farinato J., 1999, A&A, 350, L23
Ragazzoni R., Farinato J., Marchetti E., 2000, SPIE, 1076
Ribak E., 1998, SPIE, 3353, 320
Rigaut F., Gendron E., 1991, A&A, 261, 677
Spinhirne J. M. et al., 1998, SPIE, 3353, 22

This paper has been typeset from a TEX/LATEX file prepared by the author.